Constant and Variable Stiffness and Damping of the Leg Joints in Human Hopping

Svetlana Rapoport

Joseph Mizrahi
e-mail: jm@bm.technion.ac.il

Eitan Kimmel

Oleg Verbitsky

Department of Biomedical Engineering,
Technion, Israel Institute of Technology,
Haifa 32000,
Israel

Eli Isakov
Loewenstein Rehabilitation Center,
Raanana 43100,
Israel

The present study deals with the stiffness and damping profiles of the leg joints during the ground-contact phase of hopping. A two-dimensional (sagittal plane) jumping model, consisting of four linked rigid segments and including the paired feet, shanks, thighs, and the head–arms–trunk segment, was developed. The segments were interconnected by damped torsional springs, representing the action of the muscles, tendons and ligaments across the joint and of the other joint tissues. A regressive function was used to express stiffness and damping, and included second-order dependence on angle and first-order dependence on angular velocity. By eliminating redundancies in the numerical solution using multicollinearity diagnostic algorithms, the model results revealed that the correct and sufficient nonlinearity for the joint stiffness is of the first order. Damping was found negligible. The stiffness profiles obtained were bell-shaped with a maximum near mid-stance and nonzero edge values. In predicting the joint moments, the obtained variable joint stiffnesses provided a closer agreement compared to a constant stiffness model. The maximal stiffness was found to be in linear correlation with the initial stiffness in each joint, providing support to the of muscles' preactivation strategy during the flight phase of hopping. All stiffnesses increased with increasing hopping frequency. The model presented provides an effective tool for future designing of artificial legs and robots and for the development of more accurate control strategies. [DOI: 10.1115/1.1590358]

Introduction

Vertical jumping and landing is an important element in sporting and other activities. With the development of biomechanical models of human body motion, it has become possible to simulate vertical jumping in order to gain insight into intermuscular coordination and to elucidate control strategies of the musculoskeletal system. A common method to deal with this type of problems is to lump together elements of the human body, e.g., muscles, tendons, ligaments, bones, and joints so that the overall musculoskeletal system is represented as a damped elastic mechanism.

Several models describing the landing phase of running, hopping, or jumping can be found in the literature [1–6]. These models are usually characterized by the presence of elastic springs and viscous dampers, with constant properties and provide a reasonable prediction of the maximal vertical foot–ground reaction force (FGR).

In repetitive physical activity, such as in running, hopping, and trotting, the subject bounces on the ground in a spring-like manner [7–13]. Depending on the range of joint flexion and on the frequency of motion, a considerable amount of elastic energy can be stored and re-used. It has been shown that the dissipated energy in muscles increase when the amplitudes of joint movement are increased [14]. Bosco and Komi [15] also commented on the utilization of stored elastic energy stating that this depended on the shortness in latency between the stretch and shortening phases of the muscles. Accordingly, during the ground-contact period of running, hopping and trotting, the leg was modeled as a single linear spring or, in terms of the leg joints, as constant torsional springs for the ankle, knee, and hip joints, with no damping. The stiffness of these springs, termed ''average'' stiffness, was defined as the ratio between overall force or moment change to overall vertical displacement or angle change for the leg and joint stiffness, respectively [5,13].

Contributed by the Bioengineering Division for publication in the JOURNAL OF BIOMECHANICAL ENGINEERING. Manuscript received by the Bioengineering Division August 27, 2001; revision received February 26, 2003. Associate Editor: M. G. Pandy.

Physiologically, however, the conception of constant mechanical stiffness may not be applicable. For instance, muscular activation, believed to be directly related to joint stiffness, varies during the stance phase. For that reason, hopping is not a purely harmonic motion and human joints are not simple mechanical springs. Apart from its ability to store, release and absorb energy, the muscle–tendon complex can also generate energy and, as above mentioned, its stiffness generally depends on the activation level of the muscle. Thus, it can be expected that the joint stiffness is nonlinear in nature and that damping may be present and that a model accounting for these facts may improve the system's representation and model prediction [13,16].

Variations of the leg and joint stiffnesses were considered in past models as a result of variation in hopping, or stride, frequency and in ground stiffness [5,13,17–19]. It was argued that a stiffer leg leads to a higher stride frequency and shorter stride length at a given speed. Mechanical impedance variation in the subtalar joint was also considered to vary with joint angle in sudden inversion motion of the foot [20]. Rotational springs with nonlinear stiffnesses were recently studied in a three-segment leg modeling of repulsive tasks like human running and jumping [16]. No studies were found dealing with the variability of the impedances of the leg joints during the stance phase of hopping.

The main goal of the present work was to study the hypothesis that, apart from its variation with jumping frequency, the stiffness and damping of the leg joints vary also during the stance phase of hopping. The present study was thus intended to provide an insight into the mechanisms, by which the stiffness and damping are adjusted to accommodate changes taking place during the ground phase of jumping at different jumping frequencies. Studies that reproduce human motion have indicated the need for such models in prosthetics [21] in robotics [22]. Generally, leg design strategies for animals and robots rely on the range of safe operation and stiffness adjustment has been shown to extend the range of stable leg bending [16]. Additionally, control strategies based on the impedance approach require information on the continuous nonlinear

behavior of the joints [22]. Thus, the results of the present research should have implications on the design of spring based prosthetic legs and legged robots.

Methods

Experimental Procedure

Hopping Trials. Eight female subjects of average age 27 (SD, 2) years, body mass 54.8 (SD, 4.8) kg, and body height 1.63 (SD, 0.02) m, performed two-legged continuous vertical hops with the feet landing on one force platform, while keeping their hands on the waist. All the subjects were in an excellent state of health, with no previous histories of muscle weakness, neurological diseases or drug therapy. Each subject provided informed consent to participate in the study according to the University's ethical committee's guidelines.

The hops were performed at three hopping frequencies, each in a separate trial, as follows: Self-selected (or preferred frequency, PF), 18 percent lower (LF), and 18 percent higher (HF) frequency than the PF. For each individual subject the PF was determined in advance while the vertical component of the ground reaction force (GRF) was used as a means to visualize and monitor the character of the hops during the stance phase. Each subject was instructed to hop at her personal preferred frequency. The maximal deviation between the subjects was within 1.6% (see later in results). This allowed obtaining uniformity of the testing conditions and setting each of the PF (now termed middle frequency, MF), LF and HF to the same values for all the subjects. To help the jumpers keep a stable frequency, a metronome was used during the experiments to pace the hopping rhythm.

The subjects were trained prior to the experiments. All of them being not sportwomen, were demonstrated the jumping technique and were run through the experiment without data taking. In order to warm up, the subjects were requested to perform elementary gymnastic exercises. As was clearly indicated by the GRF data, the initial five hops were unstable and showed a significant deviation from the afterwards stabilized frequency and were, therefore, discarded from the data analysis. Each hopping trial started after a 10 min warmup. The trials lasted 20 s each (corresponding to approximately 37 hops in the MF), during which kinematic and force-plate data were collected. Two minutes of rest were allowed before each trial, in order to enable fatigue-free initial conditions. All the jumpers were provided with the same manufacturer and type of shoes and were carefully instructed and trained before the experiments.

Kinematic Measurements. For the kinematic measurements six-retroflective hemispherical markers of 2 cm diameter were used. The markers were located on the following sites: Two on the shoe sole (one below the lateral malleolus and one opposite to the head of the fifth metatarsal), one on the lateral malleolus, one on the lateral epicondyle of the knee, one on the tip of the greater trochanter, and one on the lateral side of the head, 5 cm above the top of the ear.

Video data were collected by a NM-M300EN Panasonic camera (50 frames/s).

The front plane of a calibration cage measuring 1.0×2.0 m was positioned on the force plate in the plane of motion and calibration was made using six control points by means of Ariel Performance Analysis System (APAS) software. The optical axis of the camera was set centrally and perpendicular to the plane of motion.

Force-plate Measurements. Three components of the GRF and the moment around the vertical axis of the force plate (KISTLER type 9281B) were recorded. The data were acquired using the LABVIEW package after they were sampled at 1000 Hz per channel.

An external trigger was used for synchronization of the force plate and the video data.

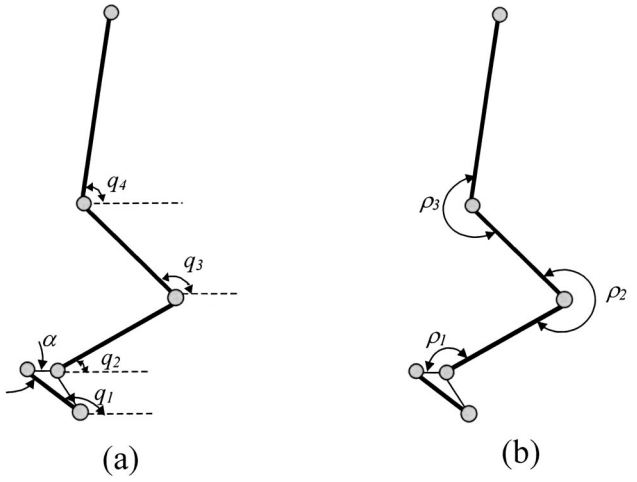

Fig. 1 Two-dimensional hopping model in the sagittal plane. (*a*) absolute angles of the joints; (*b*) anatomical angles of the joints.

Anthropometric data were estimated from body height and body mass of the subjects by using scaling methods [23].

Model

Second-order Representation of the Mechanical Impedances. A two-dimensional hopping model in the sagittal plane was used (Fig. 1), consisting of four linked rigid segments identified as the feet, shanks, thighs, and HAT (head, arms, and trunk) [24–27]. Each of the ankle, knee, and hip joints was considered to be a frictionless hinge, representing the joint action of the paired human legs. The foot was considered to establish contact with the floor through a virtual hinge located at the tip of the toe. The segments are interconnected by three mechanical impedances, representing the functional behavior of the joints [13]. Each of these impedances includes a nonlinear torsional stiffness, connected in parallel to a nonlinear torsional damper.

It was assumed that during the stance phase, motion takes place in the sagittal plane and is accomplished by pure rotation of the segments around the mentioned four joints. The kinematics of the multibody system can thus be described in terms of the absolute angles q_1, q_2, q_3, and q_4 [Fig. 1(a)] of the foot, shank, thigh, and HAT, respectively, measured from the horizontal line and represented by the generalized coordinate vector q:

$$q=[q_1 \quad q_2 \quad q_3 \quad q_4]^T \tag{1}$$

The joint angles [Fig. 1(b)] can be calculated from the absolute coordinates as follows:

$$\begin{aligned}\rho_1&=q_1-q_2+\alpha\\ \rho_2&=q_3-q_2+\pi\\ \rho_3&=q_3-q_4+\pi\end{aligned} \tag{2}$$

where ρ_j $(j=1,2,3)$ are the angles of the ankle, knee and hip, respectively, and α is the constant heel angle of the foot segment.

The mechanical properties of biological material are, in general, multiple variable-dependent. Specifically stiffness, in addition to its being nonlinear, e.g., strain dependent, often depends on the deformation rate. This is the case with bones [28], tendons and ligaments [29], cartilage [30] and muscle [31]. Similarly with damping, which can be position-dependent.

Accordingly, stiffness and damping during the stance phase of hopping are represented by a second-order regressive function, as follows:

$$K_{jl}(\rho_{jl},\omega_{jl})=k_{0j}+k_{1j}(\rho_{jl}-\rho_{j0})+k_{2j}(\rho_{jl}-\rho_{j0})^2 + k_{3j}(\omega_{jl}-\omega_{j0})$$

$$B_{jl}(\rho_{jl},\omega_{jl})=b_{0j}+b_{1j}(\omega_{jl}-\omega_{j0})+b_{2j}(\omega_{jl}-\omega_{j0})^2 + b_{3j}(\rho_{jl}-\rho_{j0}) \quad (3)$$

where the subscript $l=1,\ldots,n$ indicates a sample point and n is the total number of sample points during the stance phase; K_{jl} and B_{jl} are, respectively, the stiffness and damping of the joint j corresponding to the sample point l and k_{ij} and b_{ij}, $i=0,\ldots,3$, are coefficients to be determined from the solution. In general ρ_j and ω_j denote, respectively, the joint angle and angular velocity and ρ_{j0} and ω_{j0} are their values at the beginning of the stance phase. For simplicity, the index l is omitted in the expressions to follow.

When integrated, Eqs. (3), yield the elastic (M_{sj}) and (M_{dj}) damping torques:

$$\int_{M_{sj0}}^{M_{sjl}} dM_{sj}=\int_{\rho_{j0}}^{\rho_{jl}} K_j(\rho_j,\omega_j)d\rho_j$$

$$\int_{M_{dj0}}^{M_{djl}} dM_{dj}=\int_{\omega_{j0}}^{\omega_{jl}} B_j(\rho_j,\omega_j)d\omega_j \quad (4)$$

The total joint torque is the sum of the elastic and damping torques:

$$M_j=M_{sj}+M_{dj} \quad (5)$$

The joint torques, reaction forces and torque powers are next calculated using Newton–Eulerinverse dynamics. Then, the coefficients in Eqs. (3) can be solved from the calculated torques (τ_j) by parameter estimation using optimization procedures. Minimization of the following objective function J_j was thus performed for each of the joints (ankle, knee, and hip).

$$J_j=\sum_{l=1}^{n}(\tau_{jl}-M_{jl})^2 \quad (6)$$

Here j designates the joint and n is the length of the joint moment vector.

Model Constraints. Four inequality constraints were applied as follows. The first two assign positive values for stiffness and damping. Thus,

$$K_{jl}\geqslant 0$$

$$B_{jl}\geqslant 0 \quad (7)$$

The next constraint

$$\int_{E_{sj0}}^{E_{sjl}} dE_{sj}=\int_{\rho_{j0}}^{\rho_{jl}} M_{sj}d\rho_j'$$

$$E_{sjl}\geqslant 0 \quad (8)$$

means that the potential elastic energy E_{sj} of the spring cannot be negative, i.e., the spring cannot provide more energy than stored in it.

The last constraint precludes energy storage in the damper. Thus,

$$P_{djl}=-M_{djl}\omega_{jl}$$

$$P_{djl}\leqslant 0 \quad (9)$$

Multicollinearity Diagnostic Criteria. The model parameters should be independent of each other. Multicollinearity diagnostic criteria combined with F-test [32] were thus used to reveal dependencies and eliminate redundancies in the numerical solution of the stiffness and damping coefficients. The Hessian matrix was first formed. Its elements are the second derivatives of the objective function with respect to each of the parameters of the model.

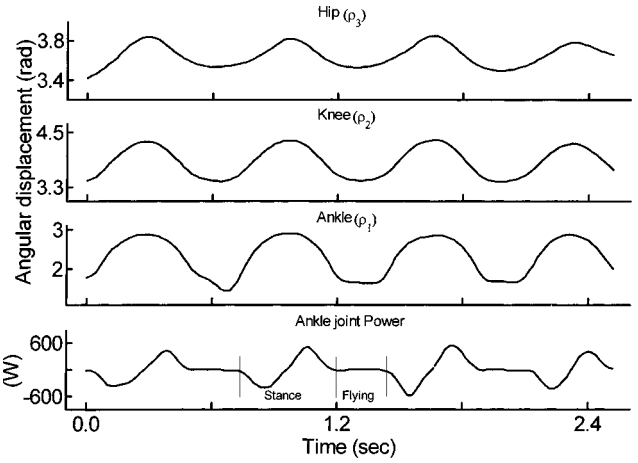

Fig. 2 Typical traces of hopping at 1.53 Hz: Joint angles are shown in the three upper traces and ankle power is shown in the lower trace

Singularity of the Hessian matrix can signify multicollinearity, i.e., relative dependence between the parameters and redundancy of information.

The following diagnostic criteria were used to indicate multicollinearity: (a) High determinant value of the Hessian; (b) high ratio between the largest eigenvalue to the smallest one; (c) existence of nonzero off-diagonal elements.

For parameter estimation to be correct all predictor variables in the multiple linear regression analysis must be uncorrelated. Thus, in case of multicollinearity, a reduction of the variables in the stiffness and damping functions should be done. Elimination of multiple collinearity was achieved by deletion of the offending predictor variable from the regression model, without impairing the ability to predict the system's response. This was done in an iterative process, while the F-test was used to examine the significance of improvement of the target function. The elements of the correlation matrix were normalized by subtracting the mean value from each data point and then by dividing by the standard deviation.

Parameter Estimation and Statistical Analysis. Parameter identification was performed by using two methods: (a) Quadratic programming (QP) [33]; and (b) genetic algorithm (GA) [34]. Comparison between the two methods by means of the t-test (with $P<0.05$). Comparison between the various testing conditions was carried out by using nonparametric Wilcoxon signed rank test for repeated measures. Statistical significance was established at $P<0.05$. The results are presented by their means and SD's.

Results

The preferred jumping frequency of all the subjects ranged between 1.84 and 1.90 Hz (average 1.87, SD 0.03 Hz). Due to the low variability between subjects LF, MF, and HF were 1.53, 1.87, and 2.20 Hz, respectively, for all the subjects.

All the subjects demonstrated a coordinated flexion–extension pattern of the ankle, knee and hip joints during the stance phase, as shown in Fig. 2. The bottom plate of this figure presents a typical power curve for the ankle joint, as computed from inverse dynamics. The amount of energy obtained in the brake (negative) phase is shown in Table 1. The brake energy was not significantly different from the push (positive) energy. It is noted from Table 1 that the highest average energy values in the brake phase were obtained in the ankle and the lowest—in the hip.

Effect of Hopping Frequency. Typical curves of the normalized vertical GRF versus the vertical excursion of the hip during the ground-contact phase are shown in Fig. 3. It is noted from

Table 1 Summary, for all subjects [Mean (SD), $n=8$], of the kinematic and kinetic results during the stance phase of hopping, at three different frequencies.

		This study			Farley & Morgenroth, 1999
Frequency (Hz)		1.53	1.87	2.20	2.20
Peak GRF (N/BW)		2.5[a] (0.3)	3.0[a] (0.3)	3.5[a] (0.4)	2.9 (0.2)
Stance time (msec)		458[a] (70)	333[a] (40)	282[a] (35)	308 (8)
Vertical excursion of hip (m)		0.27[a] (0.05)	0.22[a] (0.02)	0.18[a] (0.03)	0.121[b] (0.003)
Range of flexion (rad)	Ankle	0.85[a] (0.10)	0.69[a] (0.10)	0.59[a] (0.09)	0.56 (0.02)
	Knee	0.70[a] (0.10)	0.42[a] (0.07)	0.27[a] (0.05)	0.40 (0.04)
	Hip	0.37[a] (0.1)	0.18[a] (0.04)	0.11[a] (0.02)	0.18 (0.02)
Maximal moments (Nm)	Ankle	233.4[a] (30.1)	281.3[a] (25.6)	359.2[a] (44.1)	227 (14)
	Knee	96.8[a] (6.2)	115.3 (11.9)	123.8[a] (11.5)	150 (14)
	Hip	26.4 (6.1)	28.9[a] (3.4)	36.1[a] (4.8)	112 (24)
Brake phase energy[c] (J)	Ankle	51.8[a] (9.7)	30[a] (6.5)	21.1[a] (4.0)	…
	Knee	15.2[a] (3.7)	6.9[a] (1.9)	2.2[a] (0.7)	…
	Hip	0.7 (0.2)	0.6 (0.2)	0.4[a] (0.1)	…

[a]Denote significant differences ($P<0.05$) between Low and Medium, Medium and High, and Low and High frequencies, respectively.
[b]Denotes leg compression, expressed in m.
[c]Denotes that braking energy not significantly different than pushing energy.

these curves that, with increasing frequency, the normalized GRF increases while the vertical displacement range is reduced. Figure 4 shows typical moment/angle curves of the joints during the ground-contact phase. The joint moments were computed from inverse dynamics. The maximal moments take place at maximum joint flexion and they increase with increasing frequency. The joint moments and angular displacements were smallest in the hip, and largest in the ankle.

A summary of the average kinematic and kinetic data obtained for all the subjects in the three tested frequencies is also presented in Table 1. With increasing frequency the peak GRF increases ($P<0.05$) and the stance time decreases ($P<0.05$). During the stance phase the range of flexion of the joints and the vertical

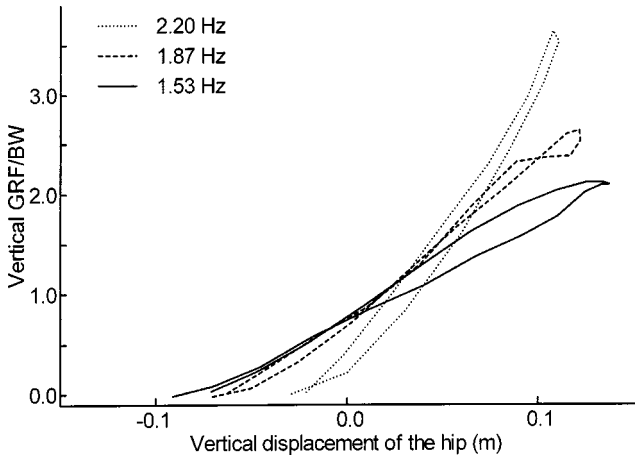

Fig. 3 Typical curves of vertical ground reaction force (GRF), normalized to body weight (BW), versus the vertical excursion of the hip during the ground-contact phase of hopping

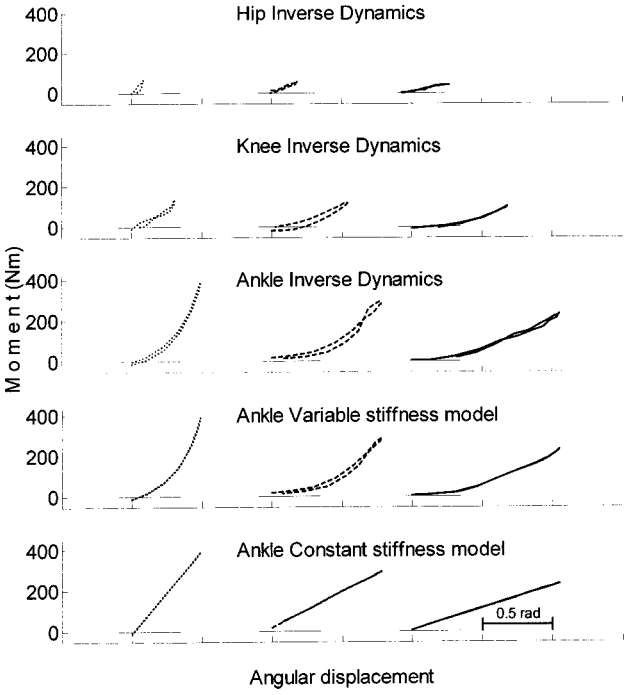

Fig. 4 Typical moment/angle curves of the leg joints during the ground-contact phase of hopping. The moments were computed from inverse dynamics for the ankle, knee and hip joints. Variable stiffness, constant stiffness model solutions are also given for the ankle joint. Left curves (dotted)=2.20 Hz; central curves (dashed)=1.87 Hz; right curves (solid)=1.53 Hz.

Table 2 Summary, for all subjects [Mean (SD), $n=8$], of stiffness of the Leg, ankle, knee and hip joints, and of the stiffness coefficients in Eq. (10).

Frequency (Hz)		This study			Farley et al., 1998	Farley & Morgenroth, 1999
Stiffness		1.53	1.87	2.20	2.20	2.20
Leg, overall ($kN\,m^{-1}$)		9.8[a] (0.4)	14.6[a] (0.8)	20.9[a] (1.1)	13.9	14.5 (0.7)
Ankle	Overall ($Nm\,rad^{-1}$)	278.8[a] (65.9)	434.3[a] (40.9)	584.8[a] (52.2)	480[c]	401 (25)
	Average ($Nm\,rad^{-1}$)	268.5[a] (66.6)	426.2[a] (87)	586.6[a] (110.2)	…	…
	k_0 ($Nm\,rad^{-1}$)	178.5[a] (32.3)	223.3[a] (57.4)	301.4[a] (63.4)	…	…
	k_1 ($Nm\,rad^{-2}$)	193.3[a] (39.7)	560.8[a] (96.0)	948.2[a] (149.4)	…	…
Knee	Overall ($Nm\,rad^{-1}$)	142.0[a] (45.4)	292.4[a] (28.9)	470.8[a] (31.8)	400[c]	368 (80)
	Average ($Nm\,rad^{-1}$)	153.2[a] (33.9)	270.6[a] (79.0)	471.6[a] (84.9)	…	…
	k_0 ($Nm\,rad^{-1}$)	110.0[a] (29.6)	158.8[a] (67.1)	230.9[a] (66.6)	…	…
	k_1 ($Nm\,rad^{-2}$)	169.3[a] (33.6)	541.3[a] (77.5)	884.8[a] (175.4)	…	…
Hip	Overall ($Nm\,rad^{-1}$)	104.1[a] (5.0)	224.4[a] (20.3)	380.6[a] (34.0)	280[c]	366 (131)
	Average ($Nm\,rad^{-1}$)	127.8[b] (50.0)	218.6[a] (52.1)	277.3[a,b] (99.4)	…	…
	k_0 ($Nm\,rad^{-1}$)	95.3[a] (37.0)	139.4[a] (31.5)	175.4[a] (28.0)	…	…
	k_1 ($Nm\,rad^{-2}$)	161.8[a] (24.1)	526.9[a] (96.6)	894.8[a] (172.3)	…	…

[a]Denote significant differences ($P<0.05$) between Low and Medium, Medium and High, and Low and High frequencies, respectively.
[b]Denotes a significant difference ($P<0.05$) between constant stiffness and variable stiffness models.
[c]Estimated from Farley et al.(1998).

excursion of the hip were found to significantly decrease with frequency. The maximum moments in the joints significantly increase with increasing frequency (see Table 1).

The slopes determined by the ratio between overall GRF, or moment change, to overall vertical displacement, or angle change, (Figs. 3 and 4) provide a measure of the 'overall stiffness' of the leg or joint, respectively. Summary of the overall leg and joint stiffnesses for all the tested subjects are presented in Table 2.

Reduction of the Model. By applying the multicollinearity diagnostic criteria and F-test, the most significant stiffness coefficients (with $P<0.05$) were k_{0j} and k_{1j} [Eqs. (3)]. The damping coefficients showed no significance, except for b_{0j}, which showed significance only in 30 percent of the subjects' jumps. Thus, we suggest reducing the optimal model to a 3-parameter model, with a linearly variable stiffness and a constant damping, as follows:

$$K_j(\rho_j)=k_{0j}+k_{1j}(\rho_j-\rho_{j0}) \tag{10}$$

$$B_j=b_{0j} \tag{11}$$

Summary of the stiffness coefficients of Eq. (10) are also presented in Table 2.

Parameter Estimation. Comparison of the two methods of parameter identification revealed that they converged to the same coefficients, approving the validity of the solution.

Stiffness/time curves were obtained by the QP optimization procedure. The stiffness behavior was similar in the ankle, knee, and hip joints (Fig. 5). As shown in this figure, nonzero stiffness values are noticed both at the touchdown and take-off instants of the stance phase. The stiffness reaches its maximum value at midstance, when the jumper's joints are maximally flexed. Direct comparison of the measured and fitted torques is demonstrated in Fig. 4. The mean value of the stiffness/time of the curve was calculated and the average for all the subjects is presented in Table 2, together with the overall joint and leg stiffnesses. The value of the damping coefficient was below 0.72 Nms/rad and the contribution of damping to the net moment did not exceed 6%. Average ankle joint moment (for all the tests) at the high frequency hopping is shown in Fig. 6. The moment was obtained by three meth-

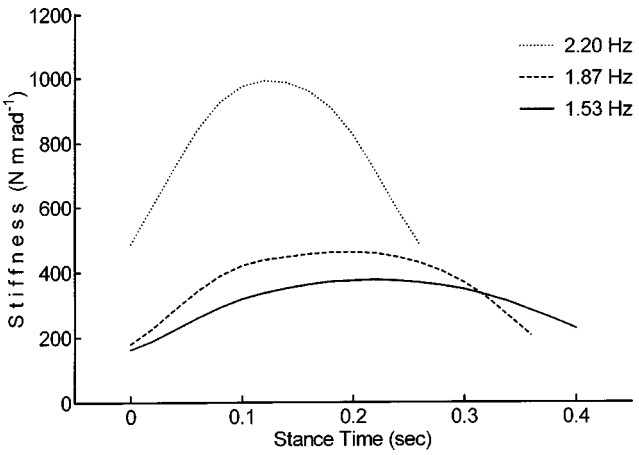

Fig. 5 Typical stiffness/time curves for the ankle during the stance phase of hopping

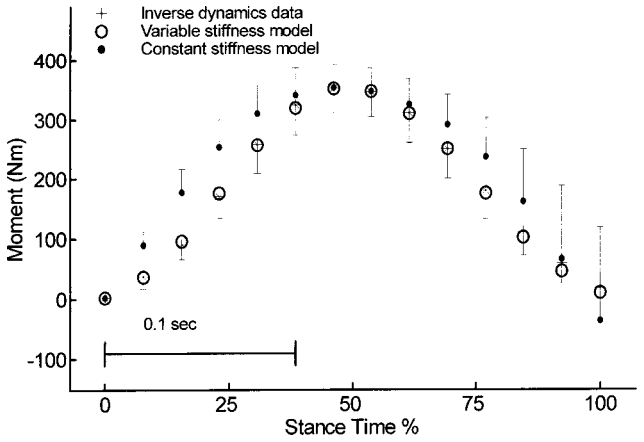

Fig. 6 Average ankle moment at 2.20 Hz hopping as obtained from three different methods: Inverse dynamics; kinematics with overall (constant) stiffness; and kinematics with actual (variable) stiffness. Standard deviations for the constant stiffness and variable stiffness moment results are indicated by the corresponding vertical bars. The difference between the moments using these two models was found significant ($P<0.05$) in points 2–5 and 10–12 along the time axis.

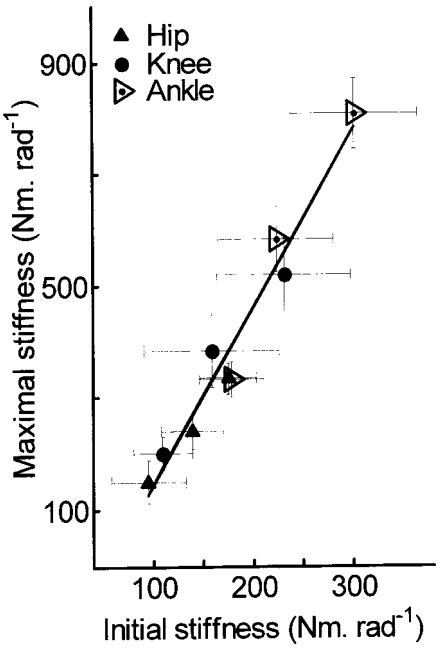

Fig. 7 Average maximal stiffness versus average initial stiffness for each of the joints and hopping frequencies

ods: (i) From inverse dynamics, (ii) prediction from kinematics and overall stiffness, and (iii) prediction from kinematics and the actual stiffness profile [Eq. (10)]. Each of the predicted solutions was compared to the solution obtained from inverse dynamics by calculating the sum of the square of the errors (SSE). The results, presented in Table 3, indicate that the constant stiffness solution was significantly different from the inverse dynamics solution, while the variable stiffness solution was not.

Figure 7 presents a plot of the average maximal stiffness versus the average initial stiffness for each of the joints and the hopping frequencies. All stiffnesses increase with increasing frequency. A straight line was found to adequately describe the correlation between the two stiffnesses ($r^2=0.95$). The horizontal and vertical bars represent the respective standard deviations and indicate that the deviations arelarger for higher frequencies.

Table 3 Comparison of the error of the joints moment over time between the Inverse Dynamics (reference) model and each of the constant stiffness and variable stiffness models [Mean(SD), $n=8$]. The values presented were calculated from the formula ($SSE\times10^{-3}$)/$N*FR$, where N is the number of points in the stance phase ($N=22$, 18, and 14 for LF, MF, and HF, respectively) and FR ($=50$) is the frame rate of the camera.

Frequency	Models	Ankle	Knee	Hip
HF	Inverse dynamics, versus Variable stiffness model	12.16 (16.21)	0.20 (0.22)	0.09 (0.10)
	Inverse dynamics, versus Constant stiffness model	239.1[a] (227.9)	39.00[a] (23.84)	21.77 (31.86)
MF	Inverse dynamics, versus Variable stiffness model	3.74 (2.66)	0.12 (0.11)	0.57 (1.01)
	Inverse dynamics, versus Constant stiffness model	95.70[a] (62.01)	88.98 (89.63)	0.81 (0.65)
LF	Inverse dynamics, versus Variable stiffness model	5.16 (4.06)	1.31 (2.57)	0.17 (0.28)
	Inverse dynamics, versus Constant stiffness model	32.05[a] (29.80)	20.41[a] (20.40)	1.44[a] (1.11)

[a]Denotes a significant difference ($P<0.05$) between the Inverse dynamics (reference) and Constant stiffness models.

Discussion

The basic outcome of this study is that joints demonstrate angle-dependent stiffness properties during the stance phase of hopping. Furthermore, the model solution provided the *form* of nonlinearity, which best described stiffness. It was found that the more general expressions in Eq. (3) for stiffness and damping are reduced to linearly variable stiffness profiles and constant, small, damping. These findings challenge previous studies on the subject, suggesting that stiffness nonlinearities can be neglected in the prediction of the FGR [5,12,17,18] and stands in line with recent studies demonstrating the importance of nonlinear stiffness in stabilizing elastic chains during dynamic loading [16]. Typically, the stiffness profiles were bell-shaped with a maximum near midstance. The stiffness of each joint at the beginning and at the end of the ground-contact phase had nonzero values. For all the frequencies studied, the maximal stiffness of each joint during the ground-contact phase, was found to be linearly proportional to the initial joint stiffness.

Several factors have been reported to affect reduction of peak forces as a result of landing impact, including initial flexion of the joints [1], range of motion [14,15], timing in multi-joint motion and synchronization between the various joints [35].

Thus, pre-programmed nonreflex muscle action during the early phase of impact would clearly help in reducing peak forces. The necessity of setting the joint angles and of tuning the stiffness before leg loading was discussed by Golhofer et al. [36]. Similarly, Aura, and Viitasalo [37] found a high correlation between pre-contact electromyogram (EMG) activity and the EMG activity in the concentric phase (brake phase) of the ground-contact period. Gerritsen et al. [26] found that muscles can reduce the vertical peak ground reaction force, due to their ability to absorb energy during impact. Recently, it has been reported that stiffness-recruitment and activation proportional to initial stiffness can be achieved by positive muscle force feedback [38]. The present study has indicated the presence of the initial joint stiffness from the stiffness profiles, suggesting that pre-activation is important in controlling the peak forces. It should be noted, however, that it did not provide direct information on the individual activity of the

various muscles in the leg. For that purpose EMG measurements should be added to and synchronized with the already measured kinematics and foot ground reaction forces.

Two stiffness measures were also calculated in this study: (i) The average stiffness from the stiffness profiles, termed ''model average,'' and (ii) the overall stiffness, obtained from the ratio between overall moment change to overall angle change in the angle/moment curves of each joint. This latter measure is similar in definition with that of previous studies [5], in which the joint stiffness was assumed constant. It is valid only in those cases where the moment peak and the angular displacement peak occur simultaneously, which was the case in the present study (see, e.g., Fig. 4). For each of the ankle and knee joints, the values of the two abovementioned stiffness measures were not different from each other (Table 2) and, therefore, either of them could be used for comparison with the variable stiffness model.

In predicting the joint moments from kinematics, the actual stiffness profile gave a closer agreement than the overall, constant, stiffness (Table 3). As to the moment maxima, it was found that the two predictions were very close to each other and were not significantly different from the moment maxima obtained from inverse dynamics. Thus, in those cases where the accurate prediction of the complete moment trajectory is not essential and only peak moments are sought, constant stiffness models are sufficiently adequate. Yet, the constant-stiffness assumption can only be regarded as a first approximation of the joint's mechanical impedance. The nonlinear model does provide more reliable representation of the stiffness characteristics and it is, therefore, viewed to be of importance for a more accurate simulation of human vertical jump. Recent works in robotics have also indicated the need for such models [22].

Our model predictions of the average stiffness and overall stiffness of the joints and of the overall stiffness of the leg are in accordance with those of previous studies [11,13]. It was shown that each of those quantities increases with the jumping frequency (Fig. 5, Table 2). Joint stiffness is dominated by muscular activation [39,40] and as the joints stiffen, they undergo smaller angular displacements during the ground-contact phase, also resulting in smaller excursion of the hip and higher leg stiffness. With all the other conditions (e.g., surface stiffness) remaining the same, an increase in joint stiffness should result in a higher peak of the impact forces (Table 1).

Of the leg joints studied, the highest moments and powers were found in the ankle. The reason can be related to the higher stiffness, the largest angular displacement and the relatively high moment arm of the GRFs, which in hopping motion act in the region of the balls of the feet. Thus, it is expected that the ankle joint is, in the motion studied here, the most important shock absorber of the leg joints. In hopping, at the instant when the feet impact the ground, a sharp deceleration occurs resulting in a ''shock wave'' that is transmitted upwards the skeletal system. We demonstrated here that with higher frequency the peak GRF increases and the stance time decreases, indicating that a higher jumping frequency is associated with a higher impact peak of the vertical GRF. In running motion previous studies have shown parallel results whereby an increase of the stride frequencies increases the shank shock acceleration [41–43]. Thus, the frequency effect obtained here is an increase in stiffness, a decrease in range of motion and a decrease in the power transmitted, supporting the expected shock increase.

While departing from the stiffness constancy concept, the model revealed that the correct and sufficient variability of the joint stiffness is of first order, as described by Eq. (10). This was obtained after eliminating redundancies in the numerical solution, using multicollinearity diagnostic algorithms, indicating that a higher order of nonlinearity is not necessary. This result should be considered meaningful in those problems where the constant stiffness representation is not sufficient and in cases where the system's representation has to be improved. The variable stiffness obtained solution also provides, through the obtained stiffness profiles, an insight into the patterns of the muscular activation in the legs' joints.

The fact that the simple model of a linearly variable stiffness can predict major features of the jumping exercise makes it an effective tool for future designing of artificial legs and robots and also for the development of more accurate control strategies.

Acknowledgments

This study was supported by the Fund for Promotion of Research at the Technion. The partial support of the Segal Foundation is also acknowledged.

References

[1] Greene, P. R., and McMahon, T. A., 1979, ''Reflex Stiffness of Man's Antigravity Muscles during Kneebends while Carrying Extra Weight,'' J. Biomech., **12**, pp. 881–891.
[2] Mizrahi, J., and Susak, Z., 1982, ''Elastic and Damping Response of the Human Leg to In Vivo Impact Forces,'' ASME J. Biomech. Eng., **104**, pp. 63–66.
[3] Ozguven, H., and Berme, N., 1988, ''An Experimental and Analytical Study of Impact Forces during Human Jumping,'' J. Biomech., **21**, pp. 1061–1066.
[4] Kim, W., Voloshin, A. S., and Johnson, S. H., 1994, ''Modeling of Heel Strike Transients during Running,'' J. Human Movement Science, **13**, pp. 221–244.
[5] Farley, C. T., Houdijk, H. H. P., van Strien, C., and Lourie, M., 1998, ''Mechanism of Leg Stiffness Adjustment for Hopping on Surfaces of Different Stiffnesses,'' J. Appl. Physiol., **85**, pp. 1044–1055.
[6] Spagele, T., Kistner, A., and Gollhofer, A., 1999, ''Modeling, Simulation and Optimization of a Human Vertical Jump,'' ASME J. Biomech. Eng., **32**, pp. 521–530.
[7] Cavagna, G. A., Sailbene, F. P., and Margaria, R., 1964, ''Mechanical Work in Running,'' J. Appl. Physiol., **19**, pp. 249–256.
[8] Cavagna, G. A., Heglund, N. C., and Taylor, C. R., 1977, ''Mechanical Work in Terrestrial Locomotion: Two Basic Mechanisms for Minimizing Energy Expenditure,'' Am. J. Physiol., **233**, pp. R243–R261.
[9] Blickhan, R., and Full, R. J., 1987, ''Locomotion Energetics of the Ghost Crab. II. Mechanics of the Center of Mass During Walking and Running,'' J. Exp. Biol., **130**, pp. 155–174.
[10] Alexander, R. McN., 1988, *The Spring in your Step: the Role of Elastic Mechanism in Human Running*, Free University Press, Amsterdam, pp. 17–25.
[11] Blickhan, R., 1989, ''The Spring-Mass Model for Running and Hopping,'' J. Biomech., **22**, pp. 1217–1227.
[12] McMahon, T. A., Cheng, G. C., 1990, ''The Mechanics of Running—How Does Stiffness Couple with Speed?,'' J. Biomech., **23**, (suppl. 1), pp. 65–78.
[13] Farley, C. T., and Morgenroth, D. C., 1999, ''Leg Stiffness Primarily Depends on Ankle Stiffness During Human Hopping,'' J. Biomech., **32**, pp. 267–273.
[14] Thys, H., 1978, ''Evaluations Indirecte de l'Energie Elastique Utilisee dans l'Impulsion des Sauts,'' Schweiz Z. Sportmed, **4**, pp. 169–177.
[15] Bosco, C., and Komi, P. V., 1979, ''Mechanical Characteristics and Fiber Composition of Human Leg Extensor Muscles,'' Eur. J. Appl. Physiol., **41**, pp. 275–284.
[16] Seyfarth, A., Gunther, M., and Blickhan, R., 2001, ''Stable Operation of an Elastic Three-Segment Leg,'' Biol. Cybern., **84**, pp. 365–382.
[17] Farley, C. T., Blickhan, R., Saito, J., and Taylor, C. R., 1991, ''Hopping Frequency in Humans: Test of How Springs Set Stride Frequency in Bouncing Gaits,'' J. Appl. Physiol., **71**, pp. 2127–2132.
[18] Farley, C. T., and Gonzalez, O., 1996, ''Leg Stiffness and Stride Frequency in Human Running,'' J. Biomech., **29**, pp. 181–186.
[19] Arampatzis, A., Bruggemann, G-P., and Metzler, V., 1999, ''The Effect of Speed on Leg Stiffness and Joint Kinetics in Human Running,'' J. Biomech., **32**, pp. 1349–1353.
[20] Mizrahi, J., Ramot, Y., and Susak, Z., 1990, ''The Passive Dynamics of the Subtalar Joint in Sudden Inversion of the Foot,'' ASME J. Biomech. Eng., **112**, pp. 9–14.
[21] Singer, E., Ishai, G., and Kimmel, E., 1995, ''Parameter Estimation for a Prosthetic Ankle,'' Ann. Biomed. Eng., **23**, pp. 691–696.
[22] Guihard, M., and Gorce, P., 2001, ''Simulation of a Dynamic Vertical Jump,'' Robotica, **19**, pp. 87–91.
[23] Winter, D. A., 1990, *Biomechanics and Motor Control of Human Movement*, Wiley, New York.
[24] Barin, K., 1989, ''Evaluation of a Generalized Model of Human Postural Dynamics and Control in the Sagittal Plane,'' Biol. Cybern., **61**, pp. 37–50.
[25] Pandy, M. G., and Zajac, F. E., 1990, ''An Optimal Control Model for Maximum-Height Human Jumping,'' J. Biomech., **23**, pp. 1185–1198.
[26] Gerritsen, G. M., Bogert, A. J., and Nigg, B., 1995, ''Direct Dynamics Simulation of the Impact Phase in Heel-Toe Running,'' J. Biomech., **28**, pp. 661–668.
[27] Selbie, W. S., and Caldwell, G. E., 1996, ''A Simulation Study of Vertical Jumping from Different Starting Postures,'' J. Biomech., **29**, pp. 1137–1146.
[28] Wright, T. M., and Hayes, W. C., 1980, ''Tensile Testing of Bone over a Wide Range of Strain Rates: Effects of Strain Rate, Micro-Structure and Density,'' Med. Biol. Eng. Comput., **14**, pp. 671–680.
[29] Peterson, R. H., Gomez, M. A., and Woo, S. L.-Y., 1987, ''The Effects of

Strain Rate on the Biomechanical Properties of the Medial Collateral Ligament: a Study of Immature and Mature Rabbits,'' Trans. of the 33rd Annual Meeting of the Orthopaedic Research Society, **12**, pp. 127.
[30] Li, J. T., Armstrong, C. G., and Mow, V. C., 1983, ''The Effects of Strain Rate on Mechanical Properties of Articular Cartilage in Tension,'' S. L-Y. Woo and R. Mates (eds.), Proc. Biomechanical Symposium ASME AMD, **56**, pp. 117–120.
[31] Herzog, W., and Leonard, T. R., 1991, ''Validation of Optimization Models that Estimate the Forces Exerted by Synergistic Muscles,'' J. Biomech., **24**(S1), pp. 31–39.
[32] Slinker, B. K., and Stanton, A. G., 1985, ''Multiple Regression for Physiological Data Analysis: the Problem of Multicollinearity,'' Am. J. Physiol., **249**, pp. 1–12.
[33] Gill, P. E., Murray, W., and Wright, M. H. 1981, *Practical Optimization*, Academic Press, Stanford University, California, pp. 177–182.
[34] Davis, L., 1991, *Handbook of Genetic Algorithms*, Van Nostrand Reinhold, New York.
[35] Luhtanen, P., and Komi, P. V., 1978, ''Segmental Contribution to Forces in Vertical Jump,'' Eur. J. Appl. Physiol., **38**, pp. 189–196.
[36] Golhofer, A., Strojnik, V., Rapp, W., and Schweizer, L., 1992, ''Behavior of Triceps Surae Muscle-Tendon Complex in Different Jumping Conditions,'' Eur. J. Appl. Physiol., **64**, pp. 283–291.
[37] Aura, O., and Viitasalo, J. T., 1989, ''Biomechanical Characteristics of Jumping,'' J. of Applied Biomechanics, **5**, pp. 89–98.
[38] Geyer, H., Seyfarth, A., and Blickhan, R., 2001, ''Proprioceptive Feedback in Running,'' *Proc XVIII Congress of the International Society of Biomechanics*, edited by R. Muller et al., Interrepro AG, Munchestein, Switzerland, pp. 208–209.
[39] Nielsen, J., Bisgård, C., Arendt-Nielsen, L., and Jensen, T. S., 1994, ''Quantification of Cerebellar Ataxia in Movements of the Hand,'' in *Biomechanics*, Seminar 8, Göteburg, Sweden, pp. 157–166.
[40] Weiss, P. L., Hunter, I. W., and Kearney, R. E., 1988, ''Human Ankle Joint Stiffness over the Full Range of Muscle Activation Levels,'' J. Biomech., **21**, pp. 539–544.
[41] Derrick, T. R., Hamill, J., and Caldwell, G. E., 1998, ''Energy Absorption of Impact during Runing at Various Stride Lengths,'' J. Med. and Sci. in Sports and Exercise, **30**, pp. 128–135.
[42] Verbitsky, O., Mizrahi, J., Voloshin, A., Treiger, J., and Isakov, E., 1998, ''Shock Transmission and Fatigue in Human Running,'' J. Appl. Biochem., **14**, pp. 300–311.
[43] Mizrahi, J., Verbitsky, O., Isakov, E., and Daily, D., 2000, ''Effect of Fatigue on Leg Kinematics and Impact Acceleration in Long Distance Running,'' J. Human Movement Science, **19**, pp. 139–151.